A GBAS Testbed to Support New Monitoring Algorithms Development for CAT III Precision Approach

B. Belabbas, T. Dautermann, M. Felux, M. Rippl, S. Schlüter, V. Wilken, A. Hornbostel, M. Meurer

German Aerospace Center (DLR. e.V.)
Institute of Communications and Navigation

Abstract

The development of new monitoring algorithms needs to have access to a platform that offers flexibility, operational evaluation facilities, test and validation capacities. DLR's GBAS test bed offers all these features with additional simulation capability. This paper illustrates these properties by showing an application of the recently developed absolute ionosphere gradient monitor by taking advantage of a network of three reference receivers located in the DLR's research airport at Braunschweig. This paper presents a first draft of an absolute ionosphere gradient monitor capable of detecting gradients from 300 mm/km to 2000 mm/km in order to fulfill the GAST-D requirements in terms of ionospheric gradient monitoring for the ground subsystem. The three receivers give the possibility to build two independent Absolute Slant Ionosphere Gradient Monitors (ASIGM). The performances achieved depend on the performances of the receivers, their relative location and the orientation of their baselines with respect to the runway direction. ASIGM with baseline in the direction of the runway provide the best observability of an ionsphere gradient that a GBAS user can experience during the approach phase (for straight-in approaches). The smaller the angle between the runway and the considered monitor baseline is, the lower the uncertainty of the gradient in the direction of the runway. Distribution of receivers parallel to the runway provides the best observability conditions. This paper gives the optimal relative location of receivers in order to achieve 100% detectability in the 300 to 2000 mm/km range of the absolute slant ionosphere gradient. Two configurations were investigated: one with 3 and another one with 4 receivers linearly distributed. The results obtained are extremely promising for the GAST-D requirements fulfillment and the corresponding architectures can easily be implemented.

Introduction

The Ground Based Augmentation System Testbed developed by DLR uses three receivers with separations of 740, 760 and 770 m from each other (see Figure 3). In this paper we explore the capabilities of the absolute ionosphere gradient monitor as proposed in [1] and adapt it for the multi receiver (>2) case. Initially, we present the dual baseline ionosphere gradient monitor and we define the variables and parameters of the problem. Then we investigate the performance achieved with the existing architecture of 3 receivers. Third, we adapt the monitor for the existing configuration of the GBAS test bed and analyze the simulation results of this configuration. Finally, in the last part of this manuscript, we investigate the special case of co-linearly distributed receivers and propose optimal separation strategies when using 3 or 4 aligned receivers. A conclusion summarizes the results obtained and gives directions of future work.

Dual baseline absolute slant ionosphere gradient monitor

The absolute slant ionosphere gradient monitor proposed in [1] is based on single frequency double difference carrier phase observations. Assuming a precise knowledge of the receivers positions (and thus their baseline separation vector), it is possible to determine double difference residual biases like the ionospheric decorrelation between 2 receivers. These biases can be estimated as long as they are not within the measurement uncertainty to an integer multiple of a wavelength. In the following, we keep the same notations as in [1] and describe the dual baseline absolute slant ionosphere gradient monitor.

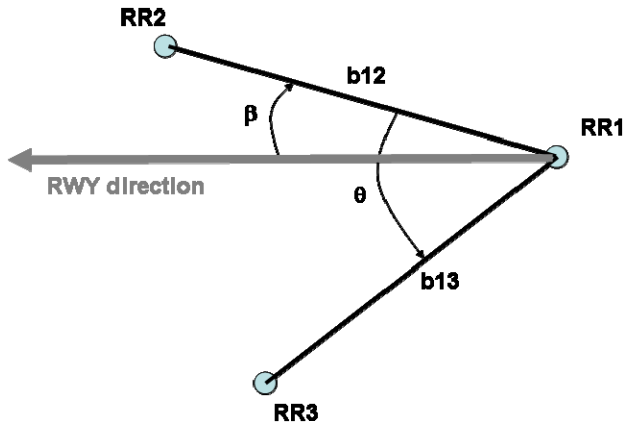

Figure 1: Configuration scheme and notations. b_{ij} is the baseline vector defined by the reference receiver RR_i and RR_j . β is the angle between b_{12} and the runway direction, θ is the angle between the two baselines

Let's denote σ_i as the standard deviation of the overbound carrier phase residual error (noise and multipath) of receiver i. In order to study the sensitivity of the monitor performances to receiver carrier phase error, we keep the standard deviation of each receiver independent and we define $r_{ij} = \sigma_j / \sigma_i$ the standard deviation ratio between receiver j and receiver i. Let's call σ_{ij} the standard deviation of the double difference phase error when considering receiver j and receiver i as reference. Then

$$\sigma_{ij} = \sqrt{2\left(1+r_{ij}^2\right)}\sigma_i \qquad (1)$$

Furthermore, we assume that the phase residual errors are independent from satellite to satellite with respect to one receiver and independent from receiver to receiver with respect to one satellite. We also assume that the errors or, more precisely, the error overbounds are Gaussian distributed.

Since our interest is to monitor the ionosphere gradient component in the direction of the runway, it is necessary to adapt the individual test statistics by projecting the baselines.

The double difference carrier phase observation equation can be written as follow (see [1]):

$$\Delta^2\phi_{ij} - \Delta\mathbf{e}^T \cdot \mathbf{b}_{ij} = \lambda\Delta^2 n_{ij} + \alpha_{ij}\left\|\mathbf{b}_{ij}\right\| + \varepsilon_{ij} \qquad (2)$$

The left hand side can be measured at each epoch and is composed of $\Delta^2\phi_{ij}$ the double difference carrier phase measurement between receiver i and receiver j, the differential receiver to satellite unit vector $\Delta\mathbf{e}^T$ (which can be determined using the navigation message of the considered satellites) and the baseline vector between the receivers $\mathbf{b}_{ij}$.

The right hand side of the equation is unknown and correspond to the sum of double difference carrier phase cycle ambiguity $\Delta^2 n_{ij}$, the ionosphere gradient α_{ij} between receiver i and j times baseline b_{ij}, and the double difference carrier phase residual error ε_{ij} whose distribution is overbounded by the Gaussian distribution with standard deviation σ_{ij} mentioned previously.

The ASIGMs measure the gradient in the baseline directions which are not necessarily aligned with the runway. Figure 2 describes this schematically:

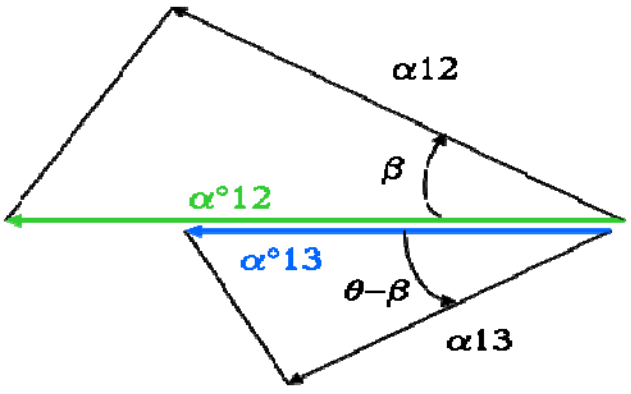

Figure 2: Ionosphere gradient projections from both monitors. α_{ij} is the gradient estimated using RR_i and RR_j and α_{ij}^o is the projection of α_{ij} in the direction of the runway. θ and β are the same angles as in Figure 1.

From Figure 2, we can see that

$$\alpha_{12}^{o} = \frac{\alpha_{12}}{\cos\beta}, \alpha_{13}^{o} = \frac{\alpha_{13}}{\cos(\theta-\beta)}. \qquad (3)$$

For each baseline, an absolute ionosphere gradient monitor using the test statistic as defined in [1] can be implemented.
We assume that these monitors are independent and that each ionosphere gradient detected by one of them is projected into the runway direction. One needs to be careful with the fact that the monitor can't observe directly the gradient in the runway direction but only the component in the direction of the baseline. An extreme case is a baseline perpendicular to the runway. This would drive to an infinite gradient when projected in the direction of the runway. Therefore the angles β and θ should be kept as close as possible to zero.

The detectable ionosphere gradients are those fulfilling the following inequalities:

$$\frac{\lambda n + (k_{ffd} + k_{md})\sigma_{12}}{b_{12}\cos\beta} < \alpha_{12}^{o} < \frac{\lambda(n+1) - (k_{ffd} + k_{md})\sigma_{12}}{b_{12}\cos\beta} \quad (3)$$

$$\frac{\lambda n' + (k_{ffd} + k_{md})\sigma_{13}}{b_{13}\cos(\theta-\beta)} < \alpha_{13}^{o} < \frac{\lambda(n'+1) - (k_{ffd} + k_{md})\sigma_{13}}{b_{13}\cos(\theta-\beta)} \quad (4)$$

with n and n' being independent integers, λ is the wavelength of the considered signal, k_{ffd} is the inflation factor for fulfilling the required probability of false alarm and k_{md} is the inflation factor for fulfilling the required probability of missed detection. Details can be found in [1].These expressions are symmetric with respect to n and n' respectively.

Application to DLR's GBAS Testbed

For our simulations, we used the actual receiver locations of the DLR's GBAS Testbed as shown in Figure 3. This GBAS Test bed is composed of 3 receivers with a plan to install a 4th one.

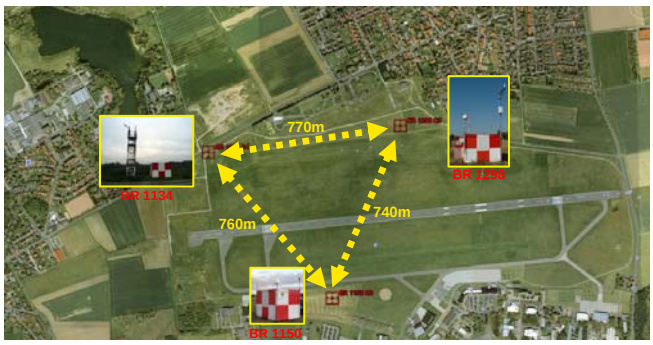

Figure 3: GBAS reference receiver location at Braunschweig airport

The locations of the receivers in ECEF coordinate system are given in Table 1:

Rx	X in m	Y in m	Z in m
RR1	3840619.039	715604.228	5024909.863
RR2	3840835.113	714861.969	5024848.587
RR3	3841202.939	715429.959	5024488.675

Table 1: Receivers' locations in ECEF coordinates

From these locations we can determine the lengths of the baselines as well as the angles between baselines and runway direction.
We consider σ_1 as a variable and for each value of σ_1 the scaling factors r_{12} and r_{13} are varying from 0.1 to 10 (carrier phase noise of RR_2 or RR_3 ranges from 10 times better to 10 times worse than carrier phase noise of RR_1). There are 2 different approaches for taking benefit of both monitors:

- A slant ionosphere gradient is considered detected if at least one monitor can detect it (minimize the missed detection probability)
- A slant ionosphere gradient is considered detected only if both monitors simultaneously detect it (minimize the false alarm probability)

These two different approaches represent exptreme cases for a commbined dual baseline monitor i.e their application gives upper and lower performance bounds.

Simulation and Analysis of Results

The sensitivity of the monitor performance with respect to the receiver accuracy is plotted in Figure 4a:

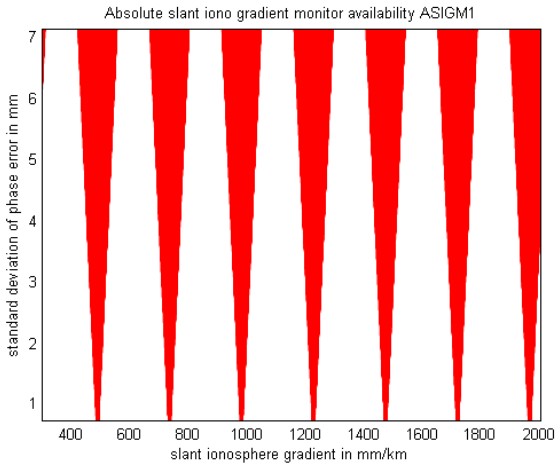

Figure 4a: Absolute slant iono gradient monitor availability function of standard deviation of phase error for baseline b_{12}. Red marks areas of slant gradient that the monitor cannot detect for a gived σ_{12}

The largest baseline b_{12} provides the largest availability at the GBAS testbed. As only the region 300-2000 mm/km is relevant for GAST-D [2], we decided to show only this area in all our results. As geometry screening [3] and [4] would induce an unacceptable level of unavailability of the system, the extreme ionosphere gradients must be monitored in an efficient way. Studies have been conducted to analyse the impact of an ionosphere monitor in GBAS applications [5] and drive to the fact that in certain circumstances an absolute ionosphere gradient is necessary.

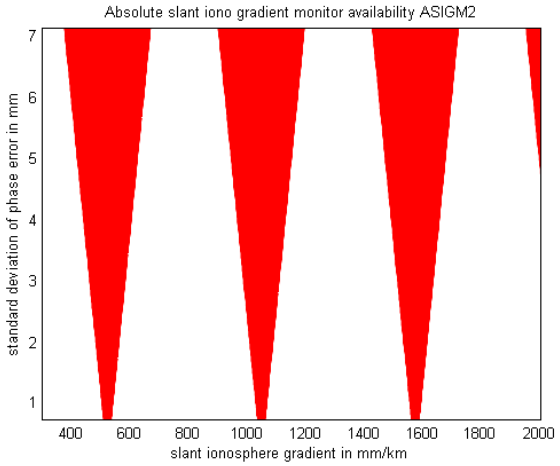

Figure 4b: Absolute slant iono gradient monitor availability function of standard deviation of phase error for baseline b_{13}.

Figures 4c and 4d show the monitor results with the logic as defined in the previous paragraph. Figure 4c shows results of detectability when both monitors can detect (represented by $\cap$) and Figure 4d demonstrates the detectability when at least one monitor can detect (represented by $\cup$)

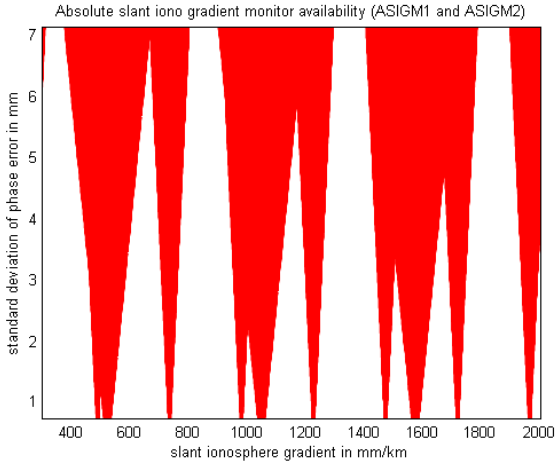

Figure 4c: $ASIGM_{12} \cap ASIGM_{13}$ detection functionality dependent on slant gradient and the level of double difference carrier phase residual error. White areas are detectable gradients.

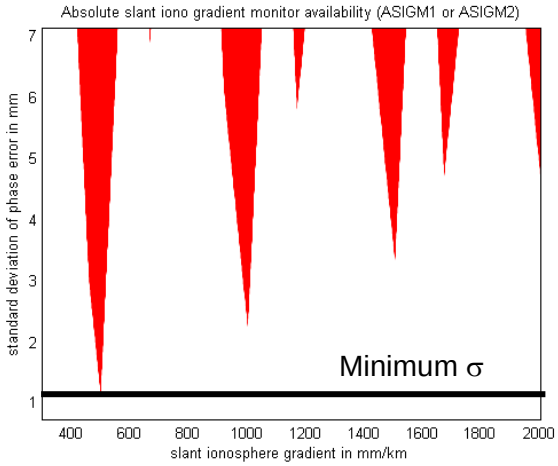

Figure 4d: $ASIGM_{12} \cup ASIGM_{13}$ detection functionality dependent on slant gradient and the level of double difference carrier phase residual error. White areas are detectable gradients.

Both Figure 4c and 4d show a loss of periodicity at least for the range of interest. The availability area is better in Figure 4d than in Figure 4c, as expected.

The impact of an additional monitor with a different baseline reduces the area of undetectability. An important aspect is the

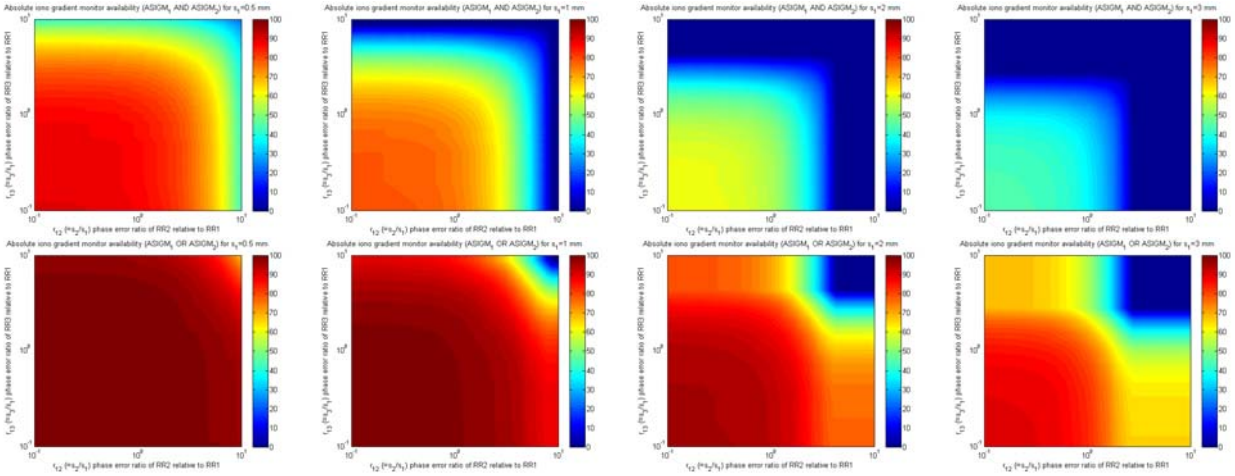

Figure **5: Percentage of detectability area (color scale from 0 to 100%) function of σ_2/σ_1 (x axis) and σ_3/σ_1 (y axis) for $ASIGM_{12} \cap ASIGM_{13}$ combination (1st raw) and for $ASIGM_{12} \cup ASIGM_{13}$ combination (2nd raw) and for σ_1 =0.5, 1, 2 and 3 mm (1st, 2nd, 3rd and 4th column)**

minimum σ for which 100% of the gradients in the range 300-2000 mm/km are detectable. This minimum σ~1 mm is shown in Figure 4d for the DLR GBAS Testbed. This is an important parameter as this will provide requirements for the antennas, receivers and level of multipath in the neighborhood of the antennas. The baseline for the additional antenna should be chosen in a way that the minimum σ that provides 100% detectability is as large as possible. From Figure 4d, an additional monitor with a maximum detectability around 500 mm/km will improve significantly the minimum allowed carrier phase double difference residual error to achieve 100% detectability.

Figure 5 shows the impact of the level of the double difference carrier phase error in the performance of a dual baseline monitor. We have on x axis the carrier phase error standard deviation ratio variation σ_2/σ_1 and on the y axis σ_3/σ_1. The colorbar represents the percentage of detectability area covered by the given configuration.
As expected the sensitivity to the reference receiver carrier phase error σ_1 is very high (colomn 1 to 4) for both configurations. We used the same axis for all plots. We can see that the curves are symmetric with respect to the line $\sigma_3 = \sigma_2$.

Optimal linear distribution of monitors

We consider in this chapter that the receivers are all aligned and parallel to the runway (co-linear). Let m be the total number of receivers with $m > 2$. Let's fix the largest baseline $b_{1m} = B$ and consider one of the receivers at the edge to be the reference receiver. Figure 7 shows a schematic description of this configuration.

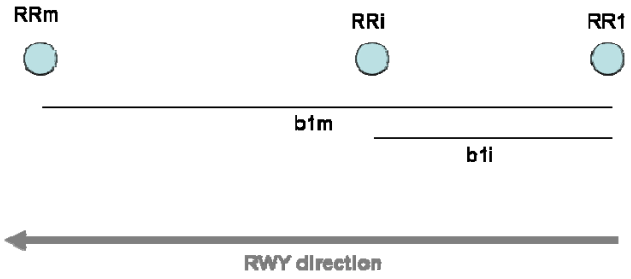

Figure 6: Schematic description of the linear distribution of receivers and notations

Suppose that the receivers have all the same performances:

$\sigma_i = \sigma_j = \frac{1}{2}\sigma \quad \forall\{i,j\} \in \{1,2,...,m\}^2$ where we have inserted the factor ½ for easier algebraic manipulation.
We define b_{1i} to be the baseline from receiver 1 to receiver i. Let's define the baseline ratio $\eta_i = b_{1i}/b_{1m}$. There are m-1 ratios to be considered with $0 = \eta_1 \le \eta_i \le \eta_m = 1$.

We would like to find the optimal η_i that allows 100% detectability in the range 300-2000 mm/km using the receivers with the highest σ values.
The availability areas of the monitor $ASIGM_{1i}$ (Absolute Slant Ionospheric Gradient Monitor between receiver RR_1 and receiver RR_i) are defined using the following inequality:

$$\frac{\lambda n+\left(k_{ffd}+k_{md}\right)\sigma}{\eta_i B}\le\alpha\le\frac{\lambda\left(n+1\right)-\left(k_{ffd}+k_{md}\right)\sigma}{\eta_i B} \quad (5)$$

α is the slant ionosphere gradient detectable by the monitor. This inequality defines the area where α is detectable.

It is defined for all integers n. We can observe that if $\sigma=0$, for any α there exist an integer n for which $\frac{\lambda n}{\eta_i B}\le\alpha\le\frac{\lambda\left(n+1\right)}{\eta_i B}$ and such an ideal monitor with no carrier phase error would have 100% detectability. The minimum of $\sigma\left(\alpha\right)$ for which we have 100% of detectability is obtained for $\alpha=\frac{\lambda n}{\eta_i B}\equiv\breve{\alpha}_n^i$. The minimum of $\sigma\left(\alpha\right)$ for which we have 0% detectability is obtained for $\sigma=\frac{\lambda}{2\left(k_{ffd}+k_{md}\right)}\equiv\hat{\sigma}$. It is interesting to notice that this is a constant. This is obtained for $\alpha=\frac{\lambda\left(n+1/2\right)}{\eta_i B}\equiv\hat{\alpha}_n^i$. The function $\sigma^i\left(\alpha\right)=g_i\left(\alpha\right)$ delimiting the area of availability of the monitor $ASIGM_{1i}$ is a periodically piecewise linear function that can be written in the following form:

$$\sigma^i\left(\alpha\right)=\frac{\hat{\sigma}}{\hat{\alpha}_n^i-\breve{\alpha}_n^i}\left(\alpha-\hat{\alpha}_n^i\right)+\hat{\sigma}\ \text{ if }\ \breve{\alpha}_n^i\le\alpha\le\hat{\alpha}_n^i \quad (6)$$

$$\sigma^i\left(\alpha\right)=\frac{\hat{\sigma}}{\breve{\alpha}_{n+1}^i-\hat{\alpha}_n^i}\left(\hat{\alpha}_n^i-\alpha\right)+\hat{\sigma}\ \text{ if }\ \hat{\alpha}_n^i\le\alpha\le\breve{\alpha}_{n+1}^i \quad (7)$$

For m=3, we keep B and η_2 as variable. We search the optimal B^* of B and η_2^* of η_2 that maximize the level of double difference carrier phase error and maintaining a 100% detectability of an absolute slant ionosphere gradient in the range 300-2000 mm/km.
A gradient must be at least detected by one monitor to be considered within the detection range by the whole system. The second possible combination (detectability when all monitors detect) is not considered in this chapter.

The optimal problem, defined through the objective function that we want to maximize is taken as the carrier phase error that provides 100 % of detectability in the range 300-2000 mm/km. The aim is to find the baselines that drive to this maximum and the value of the objective funcion at this optimum. The determination of this optimum is done numerically by considering discrete values for each baseline. The functions defined by equations 6 and 7 are calculated for each discretized baseline and for each integer values corresponding to the 300-2000 mm/km range. The monotors are then fused by taking the maximum values of the functions corresponding to each monitor for each slant ionosphere gradient. For each discrete value of the baselines we find the minimum of $\sigma\left(\alpha\right)$ for which 100% of detectability is guarantied. The results are plotted in Figure 7.

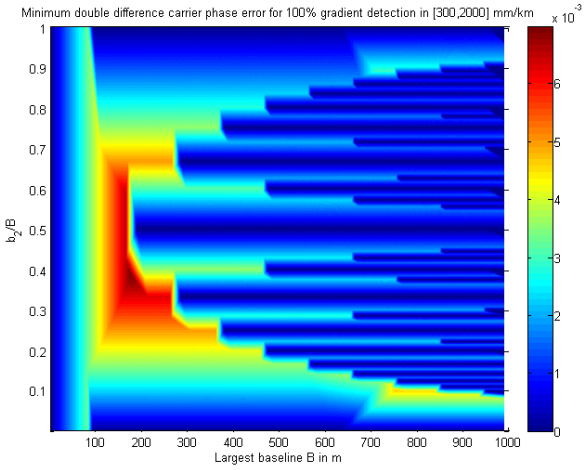

Figure 7: Maximum standard deviation carrier phase error (color scale from 0 to 7 mm) that provides 100 % detectability in the range 300-2000 mm/km function of the largest baseline in meter in the x axis and b_2/B in the y axis

We can notice in Figure 7 a superposition of symmetric trend with respect to b_2/B and a dissymmetric trend probably due to the dissymmetry of the range of slant ionopshere gradients. For B below 82 meter, there is an independancy with respect to η_2. For $B\ge190$ m and $\eta_2=0.5$ (receiver in the middle of the interval), σ takes very low values and this

architecture although symmetrical should be avoided.

The values fund for the optimum are: $\sigma^* = 6.97\ mm$, $B^* = 177\ \mathrm{m}$, $\eta_2^* = 0.387$.

This configuration provides the following detectability area:

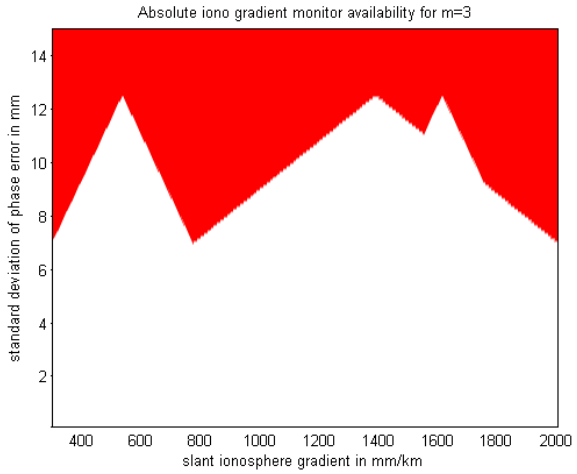

Figure 9: Slant ionosphere gradient detection area for m=3 receivers optimally linearly distributed

.

The high level of double difference carrier phase noise allowed (σ^*) can be achieved with a well calibrated antenna. The siting criteria should take into consideration the multipath environment as usual. Attention should be paid to the possible multipath correlation between RR1 and RR2 due to the shorter baseline.

If we apply these results to propose a possible location of a 4th receiver at Braunschweig research airport to achieve GAST-D requirements and consider the receivers RR1 and RR2 for the largest baseline ($B \simeq 770\ \mathrm{m}$), the optimal location for RR4 would be 77 m from RR1 and the maximum allowed double difference carrier phase error standard deviation would be 4.5 mm to achieve 100% of ionosphere gradient detectability.

For m=4 and supposing all 4 receivers are aligned. We find the following optimal surfaces:

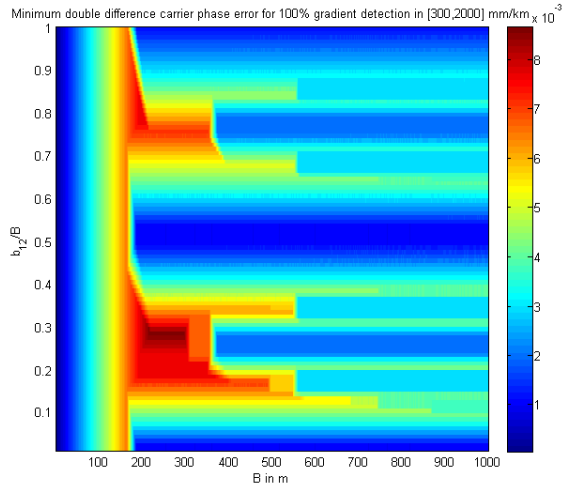

Figure 10a: Minimum carrier phase error for 100% gradient detection $\sigma_{\eta_3 *}(B, \eta_2)$

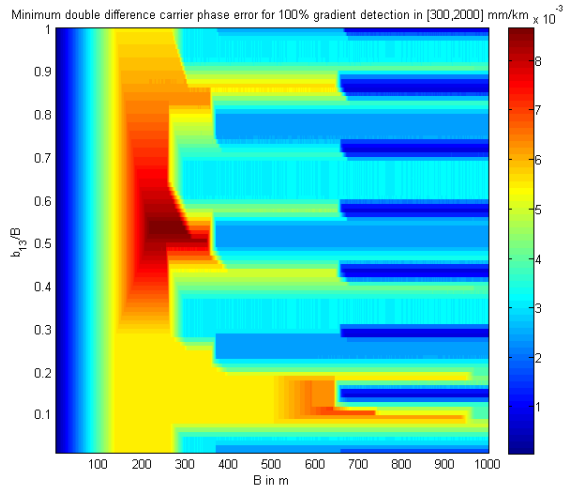

Figure 10a: Minimum carrier phase error for 100% gradient detection $\sigma_{\eta_2 *}(B, \eta_3)$

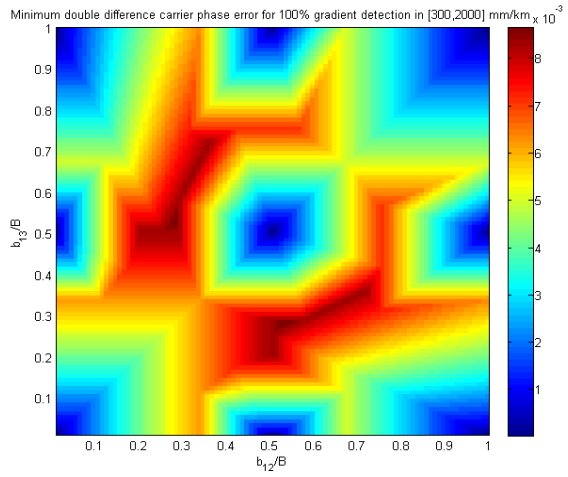

Figure 10c: Minimum carrier phase error for 100% gradient detection $\sigma_{B*}(\eta_2, \eta_3)$

The optimum is obtained for $B^* = 221\,\mathrm{m}$, $\eta_2^* = 0.28$, $\eta_3^* = 0.53$

The result is a maximum tolerable carrier phase error of $\sigma^* = 8.65\,mm$ and it provides the following detectability area:

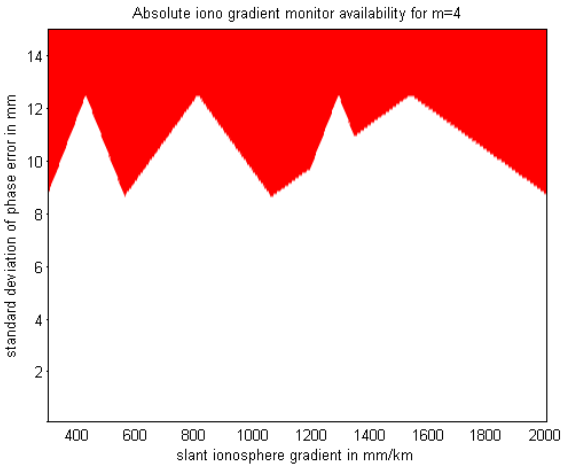

Figure 11: Slant ionosphere gradient detection area for m=4 receivers optimally distributed

As expected the addition of one receiver provides higher maximum allowable double difference carrier phase error and the maximum baseline remains acceptable for a majority of airports.

Conclusion and future work

A first analysis gives us an estimate for the maximum level of allowable carrier phase error at each receiver and an ionosphere based siting criteria for the fourth receiver in Braunschweig. The third receiver defines a baseline that is not in the direction of the runway. Therefore its test statistic can't be directly linked to a gradient that could be experienced by a ground system or an Aircraft during a CAT III precision approach. It is in that case necessary to adopt a conservative approach considering the gradient observed as the projection of a gradient in the direction of the runway. This would drive to a large number of false alarms and therefore can't fulfil the continuity requirements.
A possibility to use the non co linearity of the baselines could be in a complementary way for detecting additional characteristics of the ionosphere front like its direction. In that case additional baselines are necessary to ensure the 100% of detectability in the 300-2000 mm/km range as 2 baselines are necessary to estimate the front itself.
A linear distribution of receivers in the direction of the runway shows very promising results. The optimal distribution can be implemented in a majority of airports.

Future work consists of defining an optimal combination of individual monitors to meet overall CAT III integrity and continuity requirements validated through measurements and hardware simulations. Depending on the combination strategy, integrity and continuity allocations can be derived at each receiver level and therefore by balancing the weighting decision, it will be possible to exactly fit the overall performance requirements of the combined monitor.

References

[1] S. Khanafseh and F. Yang and B. Pervan, Carrier Phase Ionosphere Gradient Ground Monitor for GBAS with Experimental Validation, ION GNSS 2010, September 2010

[2] International Standards and Recommended Practices Aeronautical Telecommunications Annex 10, Chapter 3, Appendix B + Attachment D.

[3] Jiyun Lee and Ming Luo and Sam Pullen and Young Shin Park and Per Enge and Mats Brenner, Position-Domain Geometry Screening to Maximize LAAS Availability in the Presence of Ionosphere Anomalies, ION GNSS, 2006

[4] M. Harris and T. Murphy, Geometry Screening for GBAS to Meet CAT III Integrity and Continuity Requirements, ION NTM, January 2007

[5] M. Harris and T. Murphy, "Putting the Standardized GBAS Ionospheric Anomaly Monitors to the Test," in Proceedings of the ION GNSS 2009, Savannah, GA, Sep 2009.